

EFFECT OF DIFFERENT RIVETING SHAPE ON STRENGTH OF BONDED JOINT OF ALUMINUM POLYMER USING FEM

A.A.H. Al-Filfily A.A. Muhmmmed

*Engineering Technical College, Middle Technical University, Baghdad, Iraq
drammar@mtu.edu.iq, ayadmuhmmmed@mtu.edu.iq*

Abstract- The numerical techniques using finite element method is used to modal and analysis of bonded riveted joints utilizing different shape of rivets. The goal of this study was to recommend the best arrangement and rivet shape of these joints in order to get the most out of them. Three different rivets configuration are taken: cylindrical hole rivet, single conical rivet and double conical rivet with different rivet hole diameter 3, 4 and 5 mm. The result reveals that the maximum Von-Mises stresses occur at the center of the bonded joint on which the stress reach a peak of 84 MPa while it reduced to 14 MPa near the edge of the plate for the bonded joint only. Also, for the same rivet configuration, it is shown that the maximum stress increase when the hole diameter increases from 3 to 5 mm in the case of cylindrical hole diameter. The same behavior is observed for single and double conical rivet hole on which the stresses increase by 2.3% when the diameter rises by about 66%.

Keywords: Polymers, Riveting Joint, Bonded Materials, Abaqus.

1. INTRODUCTION

In automotive and aviation industries nowadays, it has demanded increasingly to use lightweight materials to save energy consumption and reduce pollutant emissions. The use of hybrid architectures involving polymers, composites, or metal pieces aims to take advantage of the unique properties of each material [1]. As a consequence, the nowadays modern industrial manufacturer prefers the structure that mixed between traditional metal and polymers in many real-world applications.

Joining two different materials with beneficial features such as high rigidity and strength, as well as superior resistance to fatigue and fracture damage, is, however, difficult [2]. There are different methods to fasten materials including clamping two material using screw, bolt and nut, rivets, adhesive material, and a mixture of both (mechanical and adhesive) [3].

In the automotive sector, mechanical fasteners such as rivets, pins, and bolts are extensively used. The structures that utilize hybrid methods to joint and linking composite materials have also been reported [4-7], based on extensive experimental and computational data on failure mechanisms under static and dynamic stress situations.

Due to anisotropy material behavior of these hybrid joining, the fundamental concern with these methods is that high stress riser around rivets holes reduces joint strength, which is considerably more severe and cumbersome on composite material than in metallic equivalents [8].

So, the use of adhesive method for joining two materials is more reliable than traditional mechanical method on which the loads are distributed equally and thus leads to reduce the effect of static and dynamic stress concentration factor set up in the parts to be joint [9]. These cutting-edge technologies are employed not just in aerospace but also in other technical disciplines [10].

The strength of hybrid joints can be 1.5 to 3 times that of solely glue bonded joints. Marannano and Zuccarello [11] studied the behavior of hybrid bonded/riveted joints using a numerical and experimental method. It has been shown that adding St or Al rivets to an adhesively bonded joints with an overlap length equivalent to twice the minimum size assumed by improves static strength and, more importantly, fatigue performance. Experimentally, the load capability and the ductile property of pultruded fiber-reinforced polymer for the DLJ joints with hybrid joint mechanical fasteners and adhesive material were investigated [12]. By raising the displacement rate, the ultimate failure loads of these joints were greatly enhanced, while the deformation capacity remained same.

The hybrid technique of connection with multi-directional adherends and elastic adhesive demonstrated high joint performance implying that they might increase the total safety of redundant designed structures consist of fragile pultruded fiber-reinforced polymer parts.

Habibi and Ramezani [13] conducted the influence of rivet placement on the strength and failure of nanocomposite rivet and hybrid adhesive-rivet using two experimental and computational methods. The strength of the joint rose as the number of rivets in the joint of the nanocomposite components grew, according to the results of the laboratory testing and the finite element analysis also the strength of the rivet joint is influenced by the placement of the rivets. Employing a single lap connection for cantilever beam, and double cantilever beam joints, Gupta et al. [14] investigated the strength of lap shear and fracture toughness with opening mode of epoxy/alumina nanocomposite adhesives in Al alloy joints.

The lap shear strength and fracture toughness of nanocomposite adhesives were found to be significantly higher than those of neat epoxy adhesive. Also, the glue with 1.5 wt. percent nanospheres and 1.0 wt. percent nanorods had the highest fracture toughness of both types of joint. In the present work, the FE software using Abaqus software is chose to estimate the effect of bonded layer and rivet shape on the stresses and deformation evolved in bonded joints with rivets.

2. BACKGROUND THEORY

2.1 Rivet Design

There are two main types of riveted joint: lap-joint and butt-joint. In lap joints the components to be joined overlap each other as shown in Figure 1. There are three different methods to determine the maximum tensile load that can be applied to the joint which are [15]:

1. Based on shear stress, the tensile load is given by

$$F = nA_r \tau_d \tag{1}$$

2. Based on compressive or bearing stress, the safety applied tensile load is given by

$$F = nA_b \sigma_c \tag{2}$$

$$A_b = td \tag{3}$$

3. Base on tensile strength, the tensile load is given by

$$F = A_p \sigma_t \tag{4}$$

where,

F the load (N)

A_r projected bearing area of rivet (m²)

A_b cross-sectional area of plate between rivet holes (m²)

t thickness of plate (m)

d diameter of rivet (m)

τ_d allowable shear stress MPa

σ_c allowable compressive stress MPa

σ_t allowable tensile stress MPa

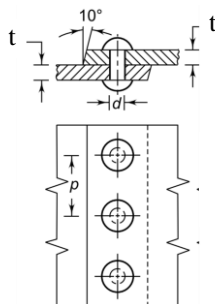


Figure 1. Single riveted lap-joint [16]

2.2. Adhesives Design

The main variables that dominate the performance of adhesive material include the nature of materials, type of adhesive and the thickness of the joint plates. The tensile stress developed in the sheet metal is given by [13]

$$\sigma = P / tw \tag{5}$$

and the shear stress is given by

$$\tau = P / Lw \tag{6}$$

3. MATERIAL PROPERTIES AND GEOMETRICAL MODELING

Ten various configurations of riveted joints with thin film adhesive layer were adopted in this research can be summarized as:

- A thin layer of adhesive material only (without rivets).
- A thin layer of adhesive material with rivets (cylindrical shape with different hole diameter $\phi 3$ mm, $\phi 4$ mm, $\phi 5$ mm).
- A thin layer of adhesive material with rivets (conical shape with different hole diameter $\phi 3$ mm, $\phi 4$ mm, $\phi 5$ mm).
- A thin layer of adhesive material with rivets (double conical shape with different hole diameter $\phi 3$ mm, $\phi 4$ mm, $\phi 5$ mm).

Figure 2 illustrates the basic dimensions of the proposed models and the applied load with the suitable constrained that mimic the real case.

The C3D8R element is used to generate the finite element meshes using eight-node brick element with reduced integration [13] through the preprocessor module, and it is frequently used in structural engineering mechanics for linear and nonlinear analysis. In addition, this element is utilized the friction model and contact boundary condition to take into account the contact surfaces between the rivet shank and the plate.

In order to have an accurate result the parts are meshed with different element number and form the coarse mesh at the outer edge of the model to fine mesh at the contact surfaces between plate and the rivet. The total number of nodes and element used for each part is shown in Table 1.

Table 1. The total number of nodes and elements used in the double cone rivet model

| Instance Name | No of Elements | No of Nodes |
|-------------------------------|----------------|-------------|
| Aluminum and polyester plates | 57942 | 67633 |
| Rivet | 5454 | 6270 |

The main assumptions used to build the numerical model in Abaqus were taken into account:

A friction factor of 0.1 was defined for the contact area between the rivet shrunk and the joint surface [17]. Half-modeling was used to reduce computation time. In addition, the perfect elastic plastic behavior of the materials was adopted in the present study. The adhesive layer is isotropic, which means that all mechanical properties in all direction are constant and the effect of flows inside the bonded material will not be included in the analysis. The applied load is assumed to be constant to better comparison between the different configuration of rivet shapes.

The physical mechanical properties of the materials used for all models are listed in Table 2. Because the displacement and hence the stresses are presumed proportionate to the load in the Abaqus program, the applied load was set to a low value of 612 N. The total number of nodes and elements are different for each method, for example 73903 nodes and 63396 elements were employed to simulate the double cone riveted-bonded FE mesh.

Figure 3 showed the central part of the joint with their rivets for three selected model (cylinder, single cone and double cone) meshed using hole diameter ($\phi 5$ mm) utilized in the present study.

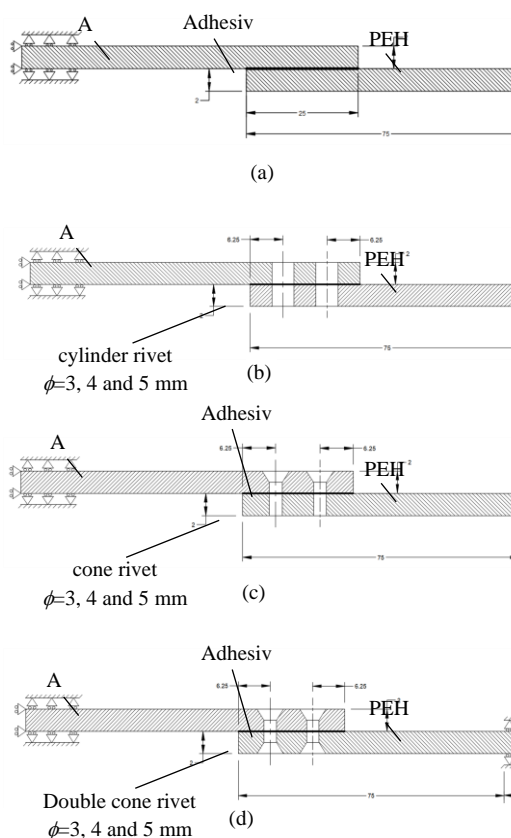


Figure 2. Geometrical configurations and applied constrain on Finite Element models of a) using adhesive material only, b) using rivets and adhesive material (cylindrical rivet), c) using rivets and adhesive material (conical rivet), d) using rivets and adhesive material (double conical rivet)

Table 2. Material parameters that were employed in this study

| Material | Elastic Modulus (GPa) | ν | Modulus of Rigidity (GPa) |
|-------------------------|-----------------------|-------|---------------------------|
| Polyester [1] | 3.1 | 0.4 | 1.1 |
| Polyethylene (PEHD) [1] | 1.5 | 0.36 | 0.75 |
| Aluminum AA1050[15] | 71 | 0.3 | 26 |

4. VALIDATION OF THE PROPOSED MODEL

In order to verify the results obtained from Abaqus software used in the current study, the case of single rivet overlap joint solved using Ansys software was taken form [18] as a verification case and comparisons are made between them. The geometry of the lap joint consists of aluminum alloy plate with a dimension of 215 mm \times 15 mm \times 2 mm and a rivet diameter of 4 mm as illustrated in Figure 4 and the material properties used for the plates and the rivet are shown in Table 3.

The finite element mesh of the geometry was done by splitting it into three parts namely outer plate, inner plate and the rivet and use dependent mesh technique. The part is fixed from the one side and the other part is allowed to move freely in the long side.

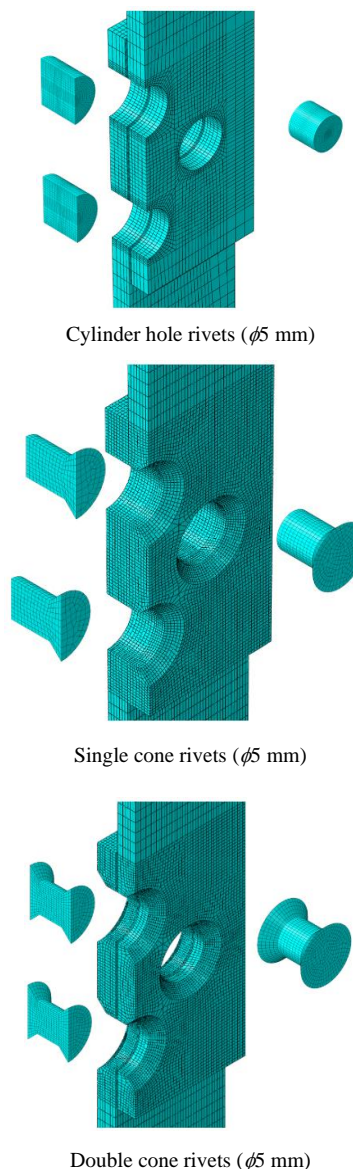


Figure 3. Mesh density for three selected models

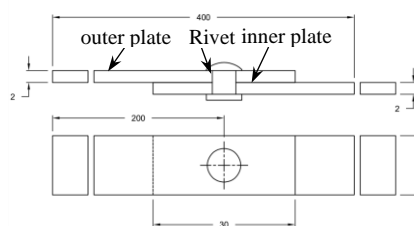


Figure 4. Actual dimension [18]

Table 3. Material properties [18]

| Material | E (Young's Modulus) | ν (Poisson's Ratio) | |
|----------|-----------------------|-------------------------|------|
| Plate | 2024-T3 | 74 GPa | 0.33 |
| Rivet | 2117-T4 | 71.7 GPa | 0.33 |

A load of 2058 N is subjected to the freely end as suggested in [18]. The contact between the head of rivet and the outer and inner surface of the plate are considered as well as between the inner hole of the outer plate and the body of the rivet.

Figure 5 shows the generated mesh of whole part with the constrained applied on it and the Figure 6 illustrate the maximum shear stress contour evaluation in the lap joint using the Abaqus. Table 4 summarizes the maximum shear stresses for both models, the present Abaqus model and the model used in [18]. It can be concluded from the table that there is a good agreement between the proposed idealization and the results obtained in [18].

Table 4. Verification results

| Type of model | Shear stress (MPa) |
|----------------------------|--------------------|
| The present model [Abaqus] | 142.32 -195.56 |
| The results of [18] | 138.44 – 184.57 |

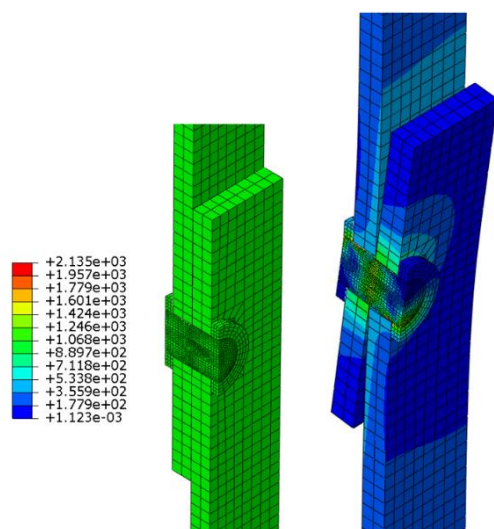


Figure 5. Idealization model using Abaqus

5. RESULTS AND DISCUSSION

The distribution of principles stresses (σ_{Mises} , σ_2 , σ_1) through the middle surface of the parts joint area in the case of using adhesive layer only are illustrated in Figure 7. It can be noticed that the maximum Von-Mises stress is raised highly in the joint area between the two plates namely Al plate and PEHD plate, when compared with the other principal stress. The Von-Mises stress reached a maximum value of 84 MPa at the mid layer of joint which reduce to 14 MPa near the outer edge of the plate as shown in Figure 7a. The calculated major and minor principal stresses (σ_1 and σ_2) are observed to be normally distribution along the bonded layer in which the maximum stress reach a value of 86 MPa near the bonded layer as indicated in Figure 7b. From Figure 7c it can be observed that the value of σ_2 is nearly 10 MPa at the mid layer since the main load is in axial direction not in the transverse direction.

Figure 8 shows the Von-Mises stress in the mid-surface of the lap riveted joint with the adhesive material for different rivet hole diameter ($\phi = 3, 4$ and 5 mm). These figures indicated that the maximum stresses occur at rivet body near the bonded layer. The maximum stresses increase by 2.4% and 4.7% in the case of hole diameter 4 and 5 mm respectively. Moreover, the maximum stresses occur at three rivets in the same time as illustrated in Figures 8a, 8b and 8c.

Figures 9 and 10 demonstrate the effect of conical rivets configuration on Mises stress for two cases single and double conical rivet. It can show that the stresses in both cases rise by 3.6, 1.2 and 1% from that of rivet with cylindrical hole. However, there is a slight difference between the stresses in single conical hole and double conical hole on which the stresses reach a maximum value of 89 MPa and 90 MPa respectively as shown in Figures 9c and 10c. Also, it can be shown from the results that the influence of the conical hole rivets has a small effect on Von-Mises stresses when compared to cylindrical rivet and one can explain that in which the slope of conical head rivet has no significant effect on stresses.

The longitudinal (along x axis) and axial (along y axis) deflections for three different cases are shown in Figures 11 and 12. It is clear that there is a small difference in a deflection between the three cases in which the transverse displacement decreased by 1.3% for single conical configuration lap joint in comparison with cylindrical lap joint as illustrated in Figures 11a and 11b. In contrast, there is a modest increase in axial deflection for double conical lap joint configuration in comparison with single conical lap joint arrangement as demonstrated in Figures 12b and 12c. Moreover, it is cleared that the value of deflection in the longitudinal direction is larger than in other direction (transverse and depth directions) on which the values increase by 28%, 29% and 30% in the case of cylindrical, conical and double conical rivet shape respectively for hole diameter of $\phi = 5$ mm and that because the load is applied in the y direction, i.e., in the direction of load as illustrated in Figures 11 and 12.

The effect of rivet hole geometry on failure modes are displayed in Figures 13a, 13b and 13c. It can be easily noticed that the mode failure in the case of cylindrical rivet hole is a pull-out mode as indicated in Figure 13a where the local yield of material occurs in the conical rivet shape (single and double) as represent in Figures 13b and 13c.

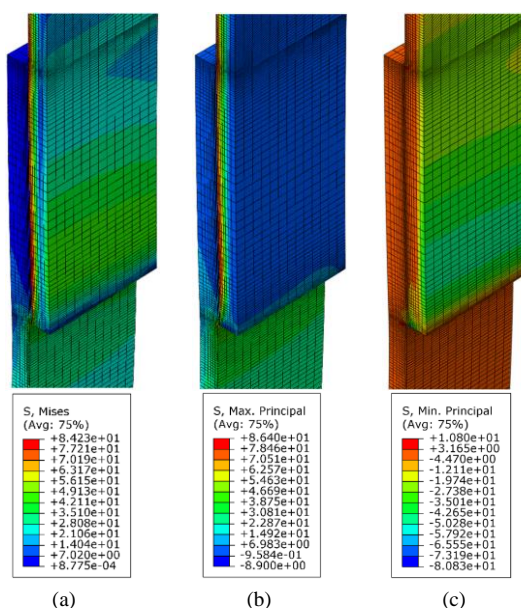


Figure 7. The distribution of stresses through the mid-layer joint: (a) Von-Mises stress, σ_{Mises} (b) Maximum principal stress, σ_1 (c) minimum principal stress, σ_2

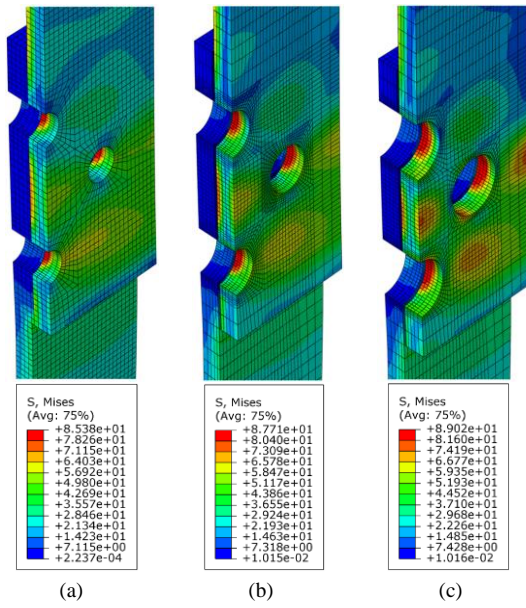


Figure 8. The distribution of Von-Mises stresses through the mid-layer of riveted bonded joint: (a) $\phi = 3$ mm, (b) $\phi = 4$ mm, (c) $\phi = 5$ mm

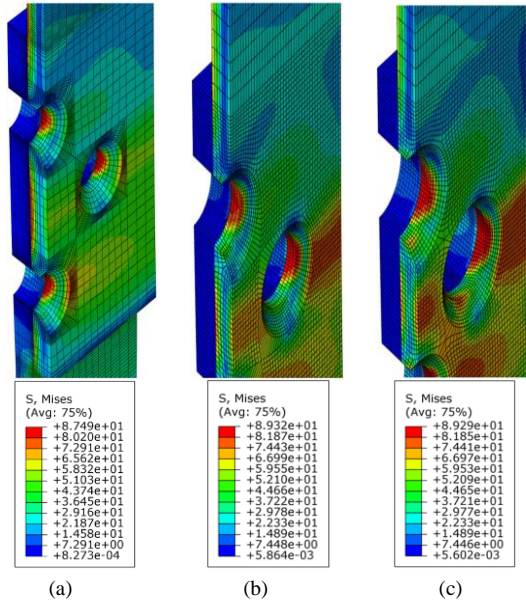


Figure 9. The distribution of Von-Mises stresses through the mid-layer of riveted bonded joint with single conical hole: (a) $\phi = 3$ mm (b) $\phi = 4$ mm, (c) $\phi = 5$ mm

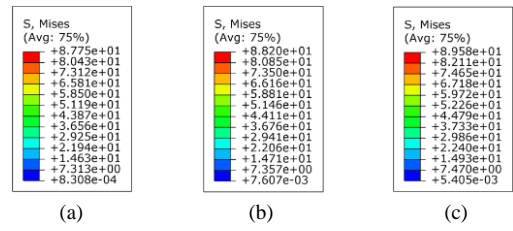
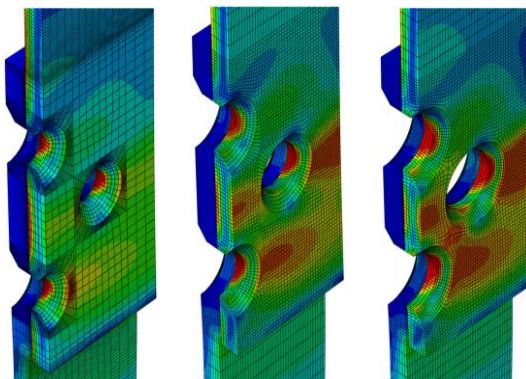


Figure 10. The distribution of Von-Mises stresses through the mid-layer of riveted bonded joint with double conical hole: (a) $\phi = 3$ mm (b) $\phi = 4$ mm (c) $\phi = 5$ mm

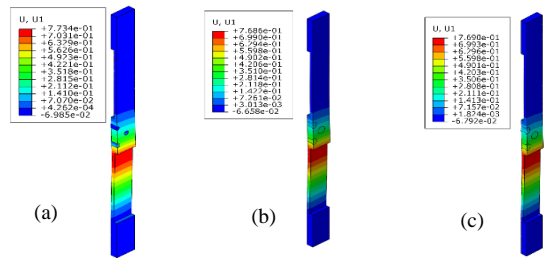


Figure 11. The contour distribution of transverse deflection for three different cases (a) cylindrical joint $\phi = 3$ mm, (b) signal conical joint $\phi = 3$ mm, (c) double conical joint $\phi = 3$ mm

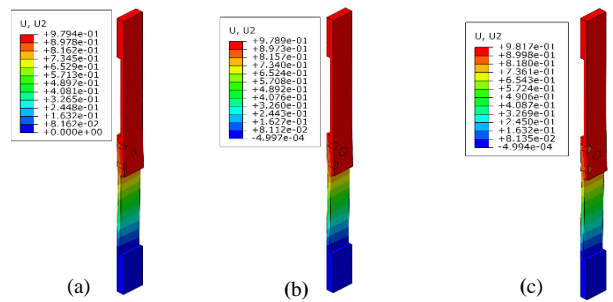


Figure 12. The contour distribution of axial deflection for three different cases (a) cylindrical joint $\phi = 3$ mm, (b) signal conical joint $\phi = 3$ mm, (c) double conical joint $\phi = 3$ mm

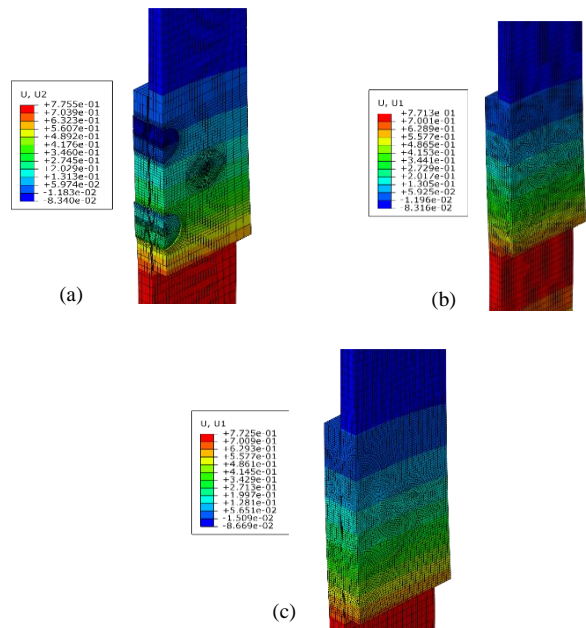


Figure 13. The contour distribution of transverse deflection for three different cases (a) cylindrical joint $\phi = 5$ mm, (b) signal conical joint $\phi = 5$ mm, (c) double conical joint $\phi = 5$ mm

6. CONCLUSIONS

The rivets bond lap joint configuration with different hole diameters ($\phi 3\text{mm}$, $\phi 4\text{mm}$, $\phi 5\text{mm}$) were carried out using numerical analysis. The maximum Von-Mises stresses occurs in the mid layer of the bonded materials for the three models studied. The cylindrical rivet configuration revealed the best design in terms of stresses and deflection. While the best design in terms of mode of failure is the double conical rivet configuration to eliminate the pull out failure mode which is noticeably seen in cylindrical rivet configuration [16].

REFERENCES

- [1] F. Lambiase, "Mechanical Behavior of Polymer-Metal Hybrid Joints Produced by Clinching Using Different Tools", *Materials and Design*, Vol. 87, pp. 606-618, 2015.
- [2] G. Di Franco, L. Fratini, A. Pasta, "Analysis of the Mechanical Performance of Hybrid (SPR/bonded) Single-Lap Joints between CFRP Panels and Aluminum Blanks", *International Journal of Adhesion and Adhesives*, Vol. 41, pp. 24-32, 2013.
- [3] G. Kelly, "Quasi-Static strength and Fatigue Life of Hybrid (bonded/bolted) Composite Single-Lap Joints", *Composite Structures*, Vol. 72, No. 1, pp. 119-129, 2006.
- [4] F. Feroldi, S. Russo, "Mechanical Performance of Pultruded FRP Plates in Beam-to-Beam Connections", *Journal of Composites for Construction*, Vol. 21, No. 4, p. 04017004, 2017.
- [5] S. Russo, "First Investigation on Mixed Cracks and Failure Modes in Multi-Bolted FRP Plates", *Composite Structures*, Vol. 154, pp. 17-30, 2016.
- [6] A. Hashimov, N. Tabatabaei, U. Samedova, M. Nuriyev, M. Bayramov, A. Mehrabov, "Microwave Absorbing Property of Epoxy Resin Composites with added Fe_3O_4 Nanoparticles", *International Journal on Technical and Physical Problems of Engineering (IJTPE)*, Issue 38, Vol. 11, No. 1, pp. 16-20, March 2019.
- [7] U.F. Samadova, A.M. Hashimov, U.M. Safarzade, I.H. Zakiyeva, A.O. Mamedov, "Influence of Filler Volume on the Magnetic Characteristics of Composites", *International Journal on Technical and Physical Problems of Engineering (IJTPE)*, Issue 48, Vol. 13, No. 3, pp. 115-118, September 2021.
- [8] G.H. Lim, K. Bodjona, K.P. Raju, S. Fielding, V. Romanov, L. Lessard, "Evolution of Mechanical Properties of Flexible Epoxy Adhesives under Cyclic Loading and its Effects on Composite Hybrid Bolted/Bonded Joint Design", *Composite Structures*, Vol. 189, pp. 54-60, 2018.
- [9] F. Moroni, A. Pirondi, F. Kleiner, "Experimental Analysis and Comparison of the Strength of Simple and Hybrid Structural joints", *International Journal of Adhesion and Adhesives*, Vol. 30, No. 5, pp. 367-379, 2010.
- [10] P. Lopez-Cruz, J. Laliberte, L. Lessard, "Investigation of Bolted/Bonded Composite Joint Behavior using Design of Experiments", *Composite Structures*, Vol. 170, pp. 192-201, 2017.
- [11] G. Marannano, B. Zuccarello, "Numerical Experimental Analysis of Hybrid Double Lap Aluminum-CFRP Joints", *Composites Part B: Engineering*, Vol. 71, pp. 28-39, 2015.
- [12] L. Liu, X. Wang, Z. Wu, T. Keller, "Resistance and Ductility of FRP Composite Hybrid Joints", *Composite Structures*, Vol. 255, p. 113001, 2021.
- [13] N. Habibi, S. Ramezani, "Experimental Study of Nanocomposite Hybrid Adhesive-Rivet Joints", *Archives of Civil and Mechanical Engineering*, Vol. 21, No. 3, pp. 1-29, 2021.
- [14] S.K. Gupta, D.K. Shukla, D. Kaustubh Ravindra, "Effect of Nanoalumina in Epoxy Adhesive on lap Shear Strength and Fracture Toughness of Aluminum Joints", *The Journal of Adhesion*, Vol. 97, No. 2, pp. 117-139, 2021.
- [15] P.R. Childs, "Mechanical Design Engineering Handbook", Butterworth-Heinemann, 2013.
- [16] V. Bhandari, "Design of Machine Elements", Tata McGraw-Hill Education, 2010.
- [17] Abaqus/ Standard User's Manual, 2021.
- [18] C. Singh, N. Kumar, "A Study on ANSYS (Workbench) Software for the Single Riveted Lap Joints", *Journal of Advances and Scholarly Researches in Allied Education* Vol. 14, No. 2, pp. 1647-1652, 2018.

BIOGRAPHIES



Ammar Ali Hussain Al-Filfily was born in Baghdad, Iraq in February 1971. He obtained the Ph.D. degree in Mechanical Engineering (Applied Mechanics) from Al-Mustansyria University, Baghdad, Iraq in 2006. He is an Assistant Professor in the field of mechanical engineering in Department of Applied Mechanics, Technical Engineering College, Middle Technical University, Baghdad, Iraq. He has published 12 papers. His scientific interests are stress analysis, die and tools, materials and welding.



Ayad Abid Muhmmmed was born in Baghdad, Iraq, in 1968. He got his M.Sc. degree in Mechanical Engineering (Applied Mechanics) from University of Turkish Aeronautical Association, Ankara, Turkey in 2017. He is an Assistant Lecturer in the field of mechanical engineering in the Department of Applied Mechanics. His current interest is focused on the improvement of adhesive strength joints, friction, tribology, materials science and die and tools design.